Jurnal Teknologi

Full Paper

INVESTIGATION OF DATUM CONSTRAINTS EFFECT IN TERRESTRIAL LASER SCANNER SELF-CALIBRATION

Mohd Azwan Abbas[a], Halim Setan[b], Zulkepli Majid[b], Albert K. Chong[c], Lau Chong Luh[b], Khairulnizam M. Idris[b], Mohd Farid Mohd Ariff[b]

[a]Faculty of Architecture, Planning & Surveying, Universiti Teknologi MARA, 02600 Arau, Perlis, Malaysia
[b]Faculty of Geoinformation & Real Estate, Universiti Teknologi Malaysia, 81310 UTM Johor Bahru, Johor, Malaysia
[c]School of Civil Engineering & Surveying, University of Southern Queensland, Australia

Article history
Received
6 April 2015
Received in revised form
12 August 2015
Accepted
23 August 2015

*Corresponding author
mohdazwan@perlis.uitm.edu.my

Graphical abstract

TLS Self-Calibration

Photogrammetry Self-Calibration

Abstract

The ability to provide rapid and dense three-dimensional (3D) data have made many 3D applications easier. However, similar to other optical and electronic instruments, data from TLS can also be impaired with errors. Self-calibration is a method available to investigate those errors in TLS observations which has been adopted from photogrammetry technique. Though, the network configuration applied by both TLS and photogrammetry techniques are quite different. Thus, further investigation is required to verify whether the photogrammetry principal regarding datum constraints selection is applicable to TLS self-calibration. To ensure that the assessment is thoroughly done, the datum constraints analyses were carried out using three variant network configurations: 1) minimum number of scan stations, 2) minimum number of surfaces for targets distribution, and 3) minimum number of point targets. Via graphical and statistical, the analyses of datum constraints selection have indicated that the parameter correlations obtained are significantly similar.

Keywords: Terrestrial laser scannesr, self-calibration, network configuration, datum constraints

Abstrak

Kemampuan untuk memberikan data tiga-dimensi (3D) dengan cepat dan padat telah menyebabkan banyak aplikasi 3D menjadi lebih mudah. Walau bagaimanapun, sama seperti peralatan optik dan elektronik yang lain, data TLS juga dipengaruhi dengan selisih. Kalibrasi-sendiri ialah kaedah yang wujud untuk menyiasat selisih tersebut bagi cerapan TLS yang mana telah diadaptasi dari teknik fotogrammetri. Tetapi, konfigurasi jaringan yang digunapakai oleh TLS dan fotogrammetri agak berbeza. Maka, siasatan lanjut diperlukan bagi memastikan samada prinsip fotogrammetri berkenaan pemilihan kekangan datum boleh digunapakai untuk kalibrasi-sendiri TLS. Bagi memastikan penilaian dibuat secara teliti, analisis kekangan datum dilaksanakan dengan tiga konfigurasi jaringan yang berbeza: 1) bilangan minimum bagi stesen cerapan, 2) bilangan minimum permukaan bagi meletakkan target, dan 3) bilangan minimum target. Secara grafik dan statistik, analisis pemilihan kekangan datum menunjukkan bahawa korelasi parameter yang diperoleh adalah signifikan sama.

Kata kunci: *Terrestrial laser scanner,*kalibrasi-senidiri, konfigurasi jaringan, kekangan datum

1.0 INTRODUCTION

Capability of terrestrial laser scanner (TLS) in three-dimensional (3D) data acquisition is not questionable, with rapid and high resolution 3D data provided, TLS has become an option for numerous applications (e.g. cultural heritage, facility management, architecture and 3D city modeling). Recently, TLS has also been utilised for accurate measurements which require millimetre geometric accuracy including landslide monitoring [1-2], structural deformation measurement [3-4], dam monitoring [5], automobile dimensioning [6] and highway clearance measurement [7], among others.

However, similar as others electronic and optical instruments, the impairing of errors in the observed data have been major causes that reduced the quality of TLS data. According to Lichti [8], there are seventeen systematic errors can be modeled in each TLS observations (e.g. range, horizontal direction and vertical angle). For quality assurance, these systematic errors have to be investigated and modelled, and subsequently applied to the raw data to improve the accuracy. There are two approaches available to investigate these errors, either separately (component calibration) or simultaneously (system calibration).

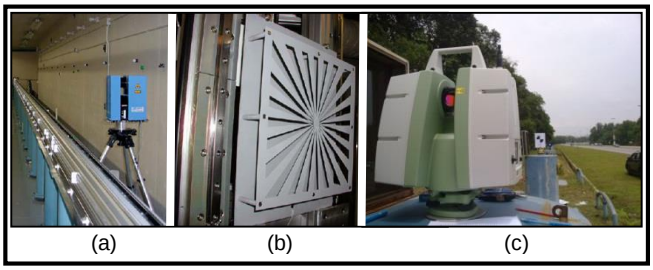

Figure 1 Facilities and devices required for component calibration, (a) Calibration trackline, (b) Targets with slots, and (c) Calibration baseline [9,10]

Due to the difficulty to provide the requirements of special laboratories and tools to performed component calibration (Figure 1), it is only implemented by academician and manufacturers. It is applicable to investigate systematic errors but most of the component calibration is used to identify the best-suited applications of the calibrated TLS and also to compare the performance of TLS from different manufacturers. In contrast, system calibration requires a room with appropriate targets to determine all significant systematic errors (Figure 5). Considering the most convenience procedure to the TLS users, system calibration which can be implemented through self-calibration was selected to investigate the systematic errors in this study.

Self-calibration used to perform system calibration was originally adapted from photogrammetry approach. Thus, similar to the photogrammetry self-calibration, the datum constraints applied for TLS self-calibration can be defined as follows: (1) minimum; and (2) inner constraints. However, according to Reshetyuk [11] both datum constraints (used in photogrammetry calibration) have their own limitations. The use of minimum constraints tends to cause large correlation between object points and some of the calibration parameters. For the inner constraints, it has unfavourable property of increasing the correlations between the calibration and exterior orientation parameters.

Analysis of correlations in self-calibration usually performed to investigate the quality of the adjustment. Though, in TLS self-calibration, the analysis focuses to reduce the correlations between calibration parameters and other system parameters. There are several causes of parameters correlation: (1) weak network geometry; and (2) the type of constraint used. Lichti [8] has reported the analysis of correlations which has indicated high correlations between calibration parameters and exterior orientation parameters as well as object points. Author assumes that weak network geometry (e.g. limitation size of calibration field and distribution of range) was the reason for that finding. With the objective to investigate the effect of constraint selection in parameters correlation for TLS self-calibration, this study will focus on the later causes.

Although self-calibration approach was adapted from photogrammetry, requirement for network configurations (e.g. targets distribution, calibration field and positions of the sensor) for the self-calibration for both TLS [8] and photogrammetry [12] are quite different. As illustrated in the Figure 2, photogrammetry self-calibration only require appropriate calibration frame with fairly distributed targets. Camera positions will be based on this frame with strong convergence [12].

Figure 2 Photogrammetry self-calibration using Photomodeler V5.0 software

While the network configuration for TLS self-calibration has been addressed by Lichti [8] as follows:

i. A large variety of ranges is needed to accurately estimate the ranging error terms, in particular the rangefinder offset;
ii. A large range of elevation angle measurements is necessary to recover some of the angular measurement error model coefficients;

iii. The self-calibration can be conducted from a minimum of two separate instrument locations provided that they have orthogonal orientation in the horizontal plane (κ angles, rotation about Z axis); and
iv. The calibration quality, as measured by reduced parameter correlations, is proportional to the number of targets used.

This argument regarding network configuration has initially indicate that the principal of datum constraints for photogrammetry is not relevant for TLS self-calibration. However, further investigation in necessity to statistically verify the effect of datum constraints to TLS self-calibration. With the intention to scrutinise this issue, this study has performed self-calibration for a Faro Photon 120 scanner. Both datum constraints were used to carry out bundle adjustment and results were statistically analysed to determine whether there is any significant difference in correlation between the calculated parameters. Furthermore, to ensure this study has critically evaluated this issue, different network configurations were adopted during experiments. Three elements were taking into account during network configurations as follows: (1) the minimum number of scan stations; (2) the minimum number of surfaces on which targets are distributed; and (3) the minimum number of point targets. As a result, analyses of datum constraints were carried out based on full networks and minimum networks configuration according to the previous three elements.

2.0 GEOMETRICAL MODEL FOR SELF-CALIBRATION

Due to the very limited knowledge regarding the inner functioning of modern terrestrial laser scanners, most researchers have made assumptions about a suitable error model for TLS based on errors involved in reflectorless total stations [8]. Since the data measured by TLS are range, horizontal and vertical angle, the equations for each measurement are augmented with systematic error correction model as follows [11]:

$$\text{Range, } r = \sqrt{x^2 + y^2 + z^2} + \Delta r \quad (1)$$

$$\text{Horizontal direction, } \varphi = \tan^{-1}\left(\frac{x}{y}\right) + \Delta\varphi \quad (2)$$

$$\text{Vertical angle, } \theta = \tan^{-1}\left(\frac{z}{\sqrt{x^2 + y^2}}\right) + \Delta\theta \quad (3)$$

Where,

x, y, z = Cartesian coordinates of point in scanner space.

Δr, Δφ, Δθ = Systematic error model for range, horizontal angle and vertical angle, respectively.

Since this study was conducted on panoramic scanners (Faro Photon 120), the angular observations computed using equation (2) and equation (3) must be modified. This is due to the scanning procedure applied by panoramic scanner, which rotates only through 180° to provide 360° information for horizontal and vertical angles as depicted in Figure 3.

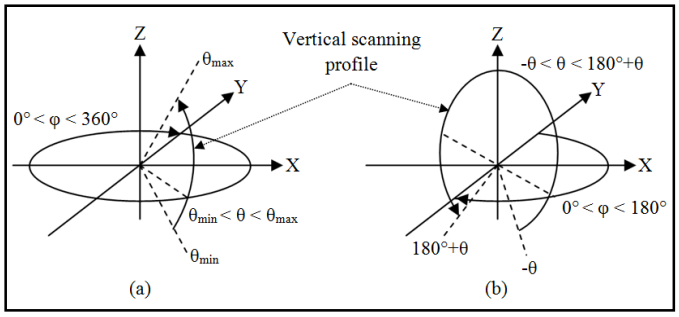

Figure 3 Angular observation ranges for (a) Hybrid scanner and (b) Panoramic scanner

Based on Lichti [13], the modified mathematical model for a panoramic scanner can be presented as follows:

$$\varphi = \tan^{-1}\left(\frac{x}{y}\right) - 180° \quad (4)$$

$$\theta = 180° - \tan^{-1}\left(\frac{z}{\sqrt{x^2 + y^2}}\right) \quad (5)$$

The modified models above, equation (4) and equation (5) are only applicable when horizontal angle is more than 180° as shown in Figure 3. Otherwise, equation (2) and equation (3) will be used, which means that panoramic scanner has two equations for both angular observations.

Regarding the systematic errors model, this study has employed the most significant errors model as applied by Reshetyuk [11] as follows:

i. Systematic error model for range.
$$\Delta r = a_0 \quad (6)$$
ii. Systematic error model for horizontal angle.
$$\Delta\varphi = b_0 \sec\theta + b_1 \tan\theta \quad (7)$$
Where,
b_0 = Collimation axis error
b_1 = Trunnion axis error
iii. Systematic error model for vertical angle.
$$\Delta\theta = c_0 \quad (8)$$

Lichti *et al*. [14] mentioned that systematic error models for panoramic scanner can be recognised based on the trends in the residuals from a least squares adjustment that excludes the relevant calibration parameters. In most cases, the trend of un-

modelled systematic error closely resembles the analytical form of the corresponding correction model. Figure 4 shows the trend of the adjustment residuals for systematic error model.

Based on Figure 4, all systematic error models are identified by plotting a graph of adjusted observations against residuals. The graph of adjusted range against its residuals (Figure 4a) will indicate a constant range error (a_0) if the trends appear like an incline line. When residuals of the horizontal observations are plotted against the adjusted vertical angles a trend like the secant function, mean that the scanner has significant collimation axis error (Figure 4b). Trunnion axis error can be identified by having a trend like tangent function as shown in Figure 4c. For vertical index error, by plotting a graph of adjusted horizontal angles against vertical angles residual, this systematic error model is considered exist when the trend looks like the big curve as depicted in Figure 4d.

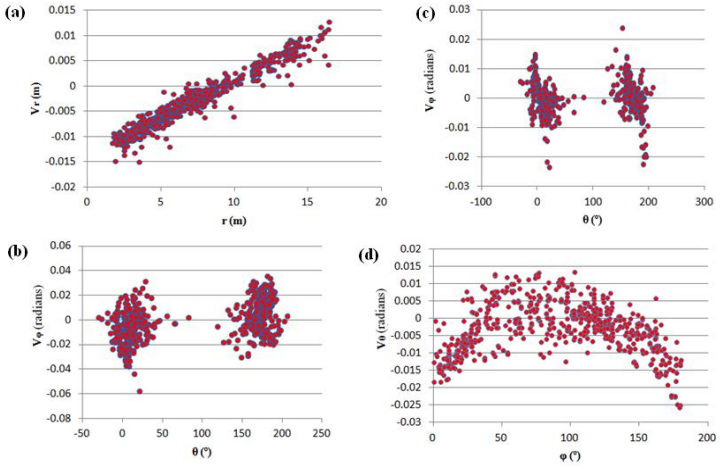

Figure 4 Systematic errors for terrestrial laser scanner, (a) Un-modelled constant error, a_0, (b) Collimation axis error, b_0, (c) Trunnion axis error, b_1 and (d) Vertical circle index error, c_0

In order to perform self-calibration bundle adjustment, the captured x, y, z of the laser scanner observations need to be expressed as functions of the position and orientation of the laser scanner in a global coordinate system [15]. Based on rigid-body transformation, for the j^{th} target scanned from the i^{th} scanner station, the equation is as follows:

$$\begin{aligned} x_i &= R_{11}(X_j - T_{Xi}) + R_{21}(Y_j - T_{Yi}) + R_{31}(Z_j - T_{Zi}) \\ y_i &= R_{12}(X_j - T_{Xi}) + R_{22}(Y_j - T_{Yi}) + R_{32}(Z_j - T_{Zi}) \\ z_i &= R_{13}(X_j - T_{Xi}) + R_{23}(Y_j - T_{Yi}) + R_{33}(Z_j - T_{Zi}) \end{aligned} \quad (9)$$

Where,

$[x_i \quad y_i \quad z_i]$= Coordinates of the target in the scanner coordinate system

${}_3R_3$ = Components of rotation matrix between the two coordinate systems for the i^{th} scanner station

$[X_j \quad Y_j \quad Z_j]$= Coordinates of the j^{th} target in the global coordinate system

$[T_{Xi} \quad T_{Yi} \quad T_{Zi}]$= Coordinates of the i^{th} scanner station in the global coordinate system.

3.0 DATUM CONSTRAINTS

Terrestrial laser scanner data involves 3D network, thus, theoretically seven datum constraints are required to remove datum defects. However, with the range observation, the scale is defined implicitly, which means that scanner network only requires six datum constraints.

To employ minimum constraints, all six datum need to be fixed. There are several procedures available to implement minimum constraints:

i. According to Reshetyuk [11], six fix coordinates distributed over 3 non-collinear points are required in order to use minimum constraints; or

ii. As applied by Gielsdorf *et al*. [16], position and orientation of one scanner station which represent by exterior orientation parameters were fixed to employ minimum constraints.

In order to use the minimum constraints, this study has fixed the exterior orientation parameters for the first scanner station. Based on the original shape of design matrix A as shown in equation (10) and equation (11), the process of removing matrix element for minimum constraints can be expressed as follows:

$${}_nA_u = [A_{EO} \quad A_{CP} \quad A_{OP}]$$

$$= \begin{bmatrix} A_{EO_1} & 0 & 0 & A_{CP1} & A_{OP_1} \\ 0 & A_{EO_2} & 0 & A_{CP_2} & A_{OP_2} \\ 0 & 0 & A_{EO_n} & A_{CPn} & A_{OP_n} \end{bmatrix}$$

Removed

(10)

Where,

n = number of observations

u = number of unknown parameters

A_{EO} = Design matrix for exterior orientation (EO) parameters

A_{CP} = Design matrix for calibration parameters (CP)

A_{OP} = Design matrix for object points (OP)

New design matrix A without EO parameters for first scanner station is in the form:

$${}_nA_u = \begin{bmatrix} 0 & 0 & A_{CP1} & A_{OP1} \\ A_{EO_2} & 0 & A_{CP2} & A_{OP_2} \\ 0 & A_{EO_n} & A_{CP_n} & A_{OP_n} \end{bmatrix} \quad (11)$$

Application of the inner constraints for this study has been adopted from Lichti [8]. The constraint imposed on object points (OP) to remove the datum defects are given in matrix form as:

$$\begin{bmatrix} 0 & 0 & G_o^T \end{bmatrix} \begin{bmatrix} \hat{X}_{EO} \\ \hat{X}_{CP} \\ \hat{X}_{OP} \end{bmatrix} = [0] \quad (12)$$

Where,

$\hat{X}_{EO}$ = Vector of the exterior orientation parameters

$\hat{X}_{CP}$ = Vector of the calibration parameters

$\hat{X}_{OP}$ = Vector of the object points

The true form of the datum design constraint matrix G_o is as follows [14].

$$G_o^T = \left(\begin{array}{ccc|ccc|ccc} 1 & 0 & 0 & 1 & 0 & 0 & 1 & 0 & 0 \\ 0 & 1 & 0 & 0 & 1 & 0 & 0 & 1 & 0 \\ 0 & 0 & 1 & 0 & 0 & 1 & 0 & 0 & 1 \\ 0 & Z_1 & -Y_1 & 0 & Z_2 & -Y_2 & 0 & Z_n & -Y_n \\ -Z_1 & 0 & X_1 & -Z_2 & 0 & X_2 & -Z_n & 0 & X_n \\ Y_1 & -X_1 & 0 & Y_2 & -X_2 & 0 & Y_n & -X_n & 0 \end{array}\right) \quad (13)$$

The bordered system of normal equation follows from the standard parametric least square is given as:

$$\begin{matrix} N & \hat{X} & + & U & = & 0 \end{matrix}$$

$$\begin{bmatrix} A^TPA & G_o^T \\ G_o & 0 \end{bmatrix} \begin{bmatrix} \hat{X}_{EO} \\ \hat{X}_{CP} \\ \hat{X}_{OP} \\ k_c \end{bmatrix} + \begin{bmatrix} A^TPL \\ 0 \end{bmatrix} = \begin{bmatrix} 0 \\ 0 \end{bmatrix} \quad (14)$$

Where,

A = Design matrix

P = Weight matrix

L = Observations matrix

k_c = Vector of Lagrange multipliers

4.0 EXPERIMENTAL

In this study, a self-calibration was performed for the Faro Photon 120 panoramic terrestrial laser scanner. The calibration was carried out in a laboratory with dimensions 15.5m (length) x 9m (width) x 3m (height). The full network configurations were adopted based on Lichti [8] conditions to ensure the quality of the obtained results.

i. The 138 black and white targets were well-distributed on the four walls and ceiling (Figure 5); and

Figure 5 Self-calibration for the Faro Photo 120 scanner

ii. Seven scan stations were used to observe the targets. As shown in Figure 6, five scan stations were located at the each corner and centre of the room. The other two were positioned close to the two corners with the scanner orientation manually rotated 90° from scanner orientation at the same corner. In all cases the height of the scanner was placed midway between the floor and the ceiling.

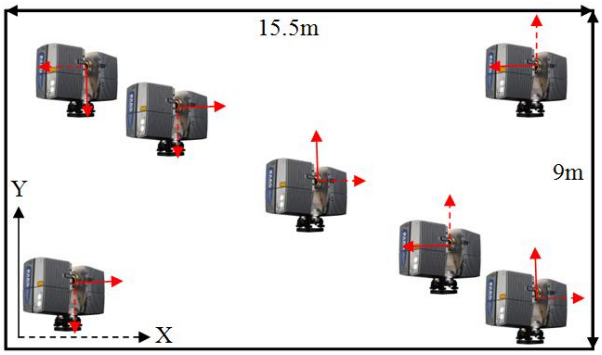

Figure 6 Scanner locations during self-calibration

With the aid of the Faroscene V5.0 software, all measured targets were extracted except for those that have high incidence angle which are not able to be recognised. A self-calibration bundle adjustment was performed using both datum constraints (e.g. inner and minimum constraints) with precision settings based on the manufacturer's specification, which were 2mm for distance and 0.009° for both angle measurements. After two iterations, the bundle adjustment process converged.

To perform datum constraints analyses, values of correlation coefficient were extracted from variance covariance matrix using the following formula [17]:

$$\rho_{xy} = \frac{\sigma_{xy}}{\sigma_x \sigma_y} \quad (15)$$

Where,

$\sigma_{x_i x_j}$: Covariance between parameters.

σ_{x_i} : Standard deviation of the parameter.

Correlations analyses were carried out between the calibration parameters and other system parameters (e.g. exterior orientation parameters and object points). To assess the significant difference in datum constraints selection, several graphs were plotted to visualise the difference between the parameter correlations of inner and minimum constraints. Furthermore, statistical analysis was performed to evaluate the results obtained from the plotted graphs. The F-variance ratio test was used to investigate the significance of the difference between two populations [18]. The null hypothesis, H_0, of the test is that the two population variances are not significantly different while the alternate hypothesis is that they are different. The F-variance ratio test is defined as:

$$F = \frac{\sigma_1^2}{\sigma_2^2} \quad (16)$$

Where,

σ_1^2 : Variance of population 1.

The null hypothesis is rejected if the calculated F value is higher than the critical F value (from the F-distribution table) at the 5% significance level. The rejection of H_0 shows that the test parameters are not equal. If the test shows no significant difference, then both datum constraints are suitable for the self-calibration bundle adjustment for terrestrial laser scanner.

With intention to investigate the concrete evidence of the effect of datum constraints selection, this study has employed several variations of network configurations as follows:

i. Full network configurations using 138 targets, all surfaces (e.g. four walls and a ceiling) and 7 scan stations.
ii. Minimum number of scan stations.
iii. Minimum number of surfaces.
iv. Minimum number of targets with seventy percent reduction.

Configuration of full network is already discussed at the earlier paragraph of this section. For the second configuration, number of scan stations was reduced from seven scan stations (Figure 6) one by one until two scan stations left as shown in Figure 7. For each time when the number of scan station reduced, the self-calibration bundle adjustment is performed and the datum constraints analyses were carried out. Results obtained will indicate any significant effect of datum constraints selection with variation of scan stations.

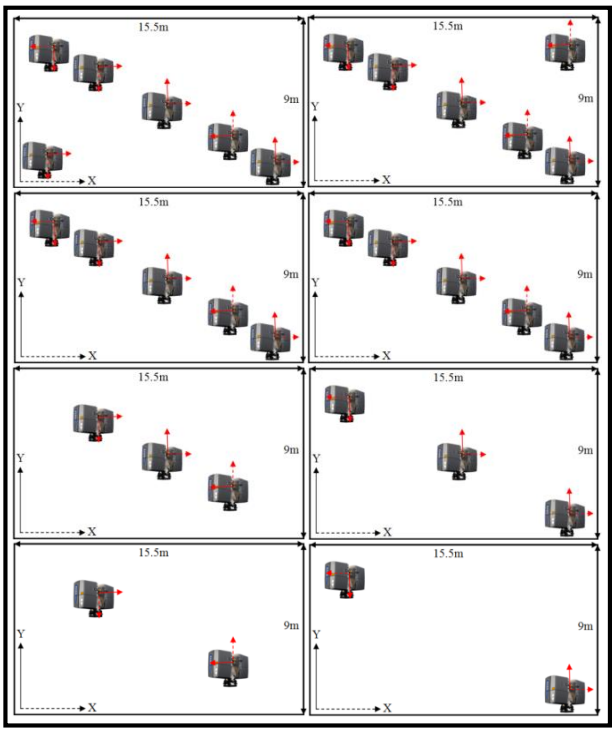

Figure 7 Reducing number of scan stations.

The subsequent configuration focuses on reducing the numbers of surfaces used for target distribution. This is very crucial due to the difficulty to get surfaces similar as laboratory condition for on-site application. In laboratory, all targets can be distributed to all walls, a ceiling and a floor but for on-site situation, sometimes there are only two walls and a floor available. In this study, four walls and a ceiling were used to distribute all 138 targets. From these five surfaces, experiment is carry out by removing those surfaces on by one until two surfaces left as shown in Figure 8. For each removing procedure, self-calibration bundle adjustment will be performed and followed with datum constraints analyses.

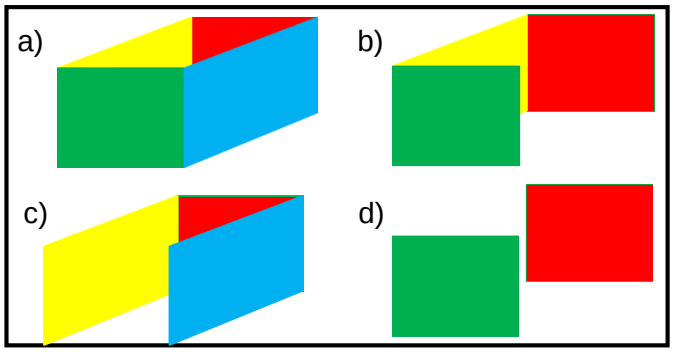

Figure 8 Reducing number of surfaces for targets distribution, (a) Four surfaces by removing a ceiling, (b) Three surfaces by removing a ceiling and a length wall, (c) Three surfaces by removing a ceiling and (d) A width wall and two surfaces

The final network configuration is carried out to investigate minimum number of targets which are suitable for TLSs self-calibration. This experiment is implemented by reducing the targets for every ten percent until seventy percent by taking into account the target distribution condition. As applied in the previous experiments, each time when the targets reduced, self-calibration bundle adjustment is carried and followed with datum constraints analyses.

5.0 RESULTS AND DISCUSSION

5.1 Self-Calibration of Faro Photon 120

Since Faro Photon 120 scanner using panoramic field of view, thus, the residual patterns of a bundle adjustment can be employed to investigate the systematic error trends. As a result, other than statistical analysis, observation residual patterns are also used for significant analysis. After performing the bundle adjustment process without any calibration parameters, residual patterns were plotted as a function of the adjusted observations as shown in Figure 9 until Figure 11.

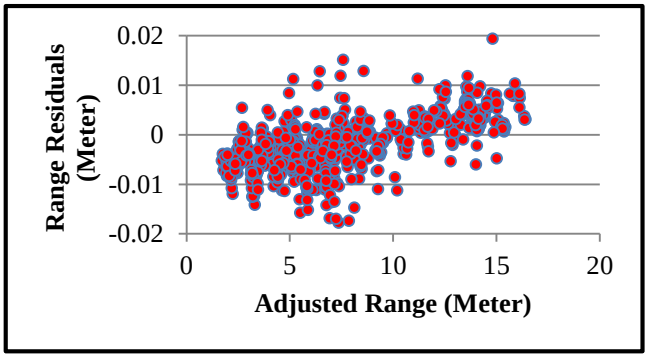

Figure 9 Range residuals as a function of adjusted range for the adjustment without calibration parameters

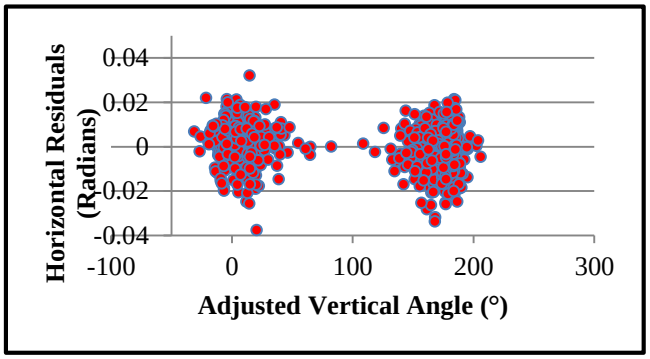

Figure 10 Horizontal angle residuals as a function of adjusted vertical angles for the adjustment without calibration parameters

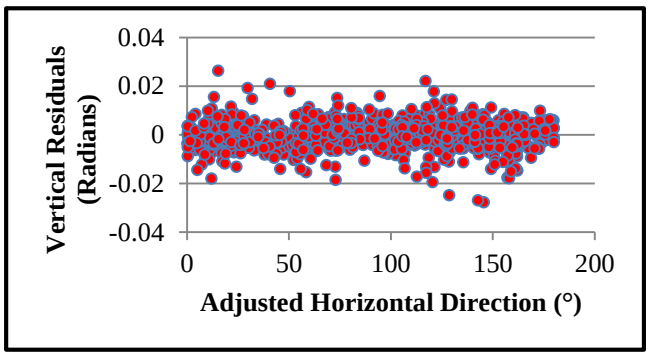

Figure 11 Vertical angle residuals as a function of adjusted horizontal angles for the adjustment without calibration parameters

Based on the sample of residual patterns shown in Figure 4, all significant systematic errors were investigated using the graphs from Figure 9 to Figure 11. There are no systematic errors exhibited in both horizontal and vertical angles observations except for the range. The residual pattern graph has obviously demonstrated the trend of inclining line. Further analysis has been performed by running the bundle adjustment again using the calibration parameters. Results of the calibration parameters for both datum constraints are shown in Table I.

Table I Calibration parameters and their standard deviations

Calibration parameters	Unit	Inner constraints	Minimum constraints
Constant range (a_0)	mm	9.3 ± 0.2	9.3 ± 0.2
Collimation axis (b_0)	"	-1.1 ± 2.1	-1.1 ± 2.1
Trunnion axis (b_1)	"	2.9 ± 8.0	2.9 ± 8.0
Vertical circle index (c_0)	"	9.4 ± 2.8	9.4 ± 2.8

Table II presents the RMS of residuals for each observable group for the cases without and with the self-calibration. The results of RMS have shown the improvement in precision up to 29% by implementing self-calibration procedure.

Table II RMS of residuals from the adjustments without and with calibration parameters

Observable	RMS (without)	RMS (with)	Improvement in percentage
Range	5.6mm	4.0mm	29%
Horizontal direction	41.0"	37.1"	10%
Vertical angle	24.0"	22.4"	7%

In order to have a concrete solution regarding the significant of the estimated systematic error model, statistical tests were performed. All calibration parameters were tested to investigate their significant. The null hypothesis, H_0, of the test is that the parameter is not significant, otherwise the hypothesis indicate that parameter is significant. Using 95% confidence level, the results of the test are shown in Table III.

Table III Significant test for calibration parameters parameters

Number of scanner stations		**7**
Degree of freedom		**1925**
Critical value for 't' (95%)		**1.645**
Calibration parameters	**Calc. 't'**	**Significant Test**
Constant range (a_0)	46.5	Significant
Collimation axis (b_0)	0.524	Not Significant
Trunnion axis (b_1)	0.363	Not Significant
Vertical circle index (c_0)	3.357	Significant

According to Table III, the null hypothesis was accepted when the calculated (Calc.) 't' is smaller than critical 't' and vice versa. The results obtained show that null hypothesis was rejected for parameter of constant rangefinder offset (a_0), and vertical circle index (c_0) parameters. This indicates that those parameters are significant. For the collimation axis (b_0) and trunnion axis (b_1) errors, the null hypothesis has been accepted.

5.2 Datum Constraints Analyses

As discussed in Section 1, one of the causes of parameters correlation is the type of constraints used. Furthermore, Reshetyuk [11] did mention that selection of datum constraints can results different types of parameters correlation in photogrammetry application. Thus, investigation is carried to ensure whether that principal is applicable for TLS self-calibration. Through graphical and statistical analysis, the results obtained are discussed in detail.

Below are the plotted graphs (Figure 12 until Figure 16) illustrated the comparison of parameters correlation between inner and minimum constraints. Due to the large number of parameters involved (e.g. seven scan stations, four calibration parameters and 138 targets) in variance covariance matrix, then this study has used mean values.

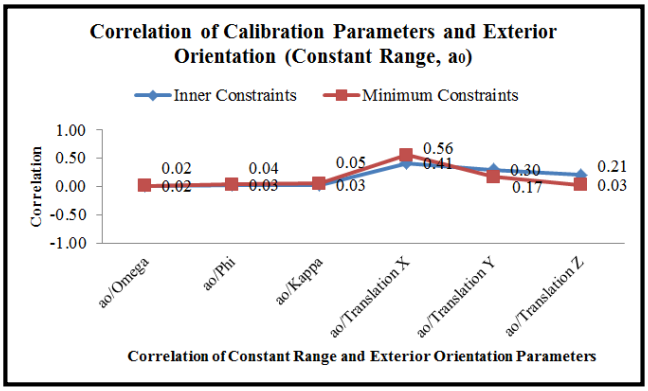

Figure 12 Parameter correlations of constant range and exterior orientation parameters (full network configuration)

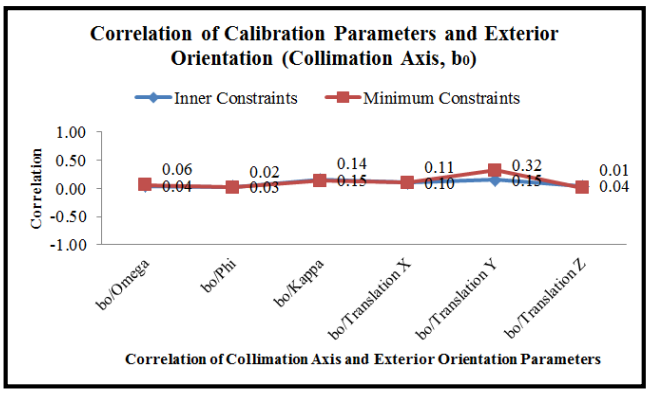

Figure 13 Parameter correlations of collimation axis and exterior orientation parameters (full network configuration)

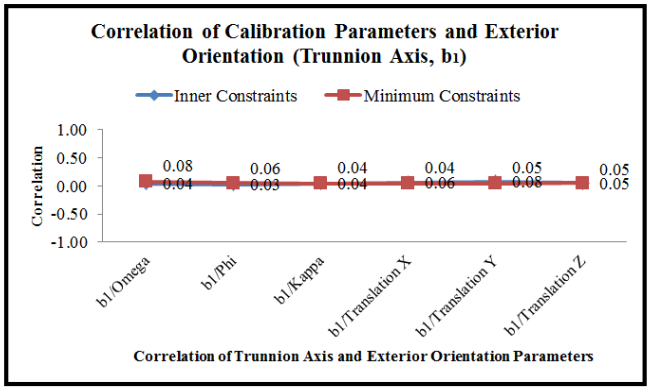

Figure 14 Parameter correlations of trunnion axis and exterior orientation parameters (full network configuration)

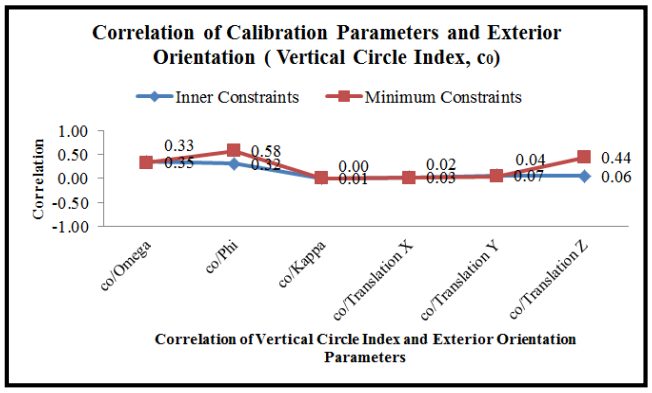

Figure 15 Parameter correlations of vertical circle index and exterior orientation parameters (full network configuration)

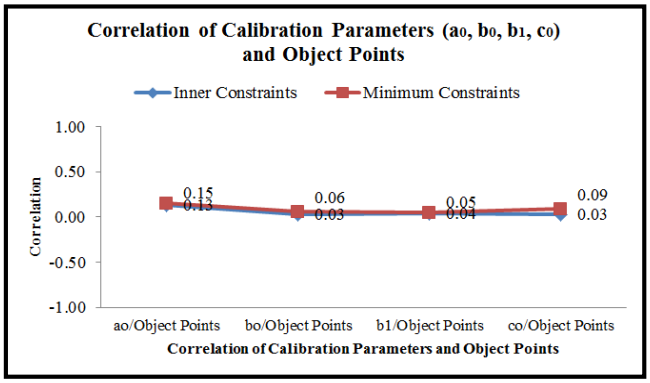

Figure 16 Parameter correlations of calibration parameters and object points (full network configuration)

Figure 12 to Figure 15 represent the plotted correlation between four calibration parameters (e.g. constant range, collimation axis, trunnion axis and vertical circle index) and exterior orientation (EO) parameters (e.g. omega, phi, kappa, translation X, translation Y and translation Z). While Figure 16 is illustrate the correlation of calibration parameters and object points. In each figure, correlations of both datum constraints are attached for visually examine the difference. However, initial conclusion can be made that there are no significant differences between datum constraints as well as the values of correlations are consider small with maximum number is 0.58 (between vertical circle index and phi in Figure 15). Through statistical analysis, F-variance ratio test has mathematically proved the similarity of results obtained.

Table IV F-variance ratio test for full network configuration

Parameter Correlations	Calculated F	>/<	Critical F
a_0 / EO	0.09	<	5.05
b_0 / EO	0.42	<	5.05
b_1 / EO	0.01	<	5.05
c_0 / EO	0.69	<	5.05
CP / OP	0.01	<	9.28

Table IV shows that in all cases, with 95% confidence level, the calculated F is smaller than critical F, which indicates the acceptation of null hypothesis (H_0). Since this is the results of full network which have employed very strong network geometry, thus, the good findings is expected.

With intention to investigate the robust conclusion regarding similarity of the correlation results yielded from both datum constraints, this study has carried out similar analysis for different type of network configurations. The first configuration is by reducing the number of scan stations. For each stations configuration, statistical analysis is performed as depicted in Table V.

Table V F-variance ratio test for different stations configurations

Configuration	Parameter Correlations	Calculated F	>/<	Critical F
6 Stations	a_0 / EO	0.07	<	5.05
	b_0 / EO	0.18	<	5.05
	b_1 / EO	0.16	<	5.05
	c_0 / EO	0.71	<	5.05
	CP / OP	0.86	<	9.28
5 Stations	a_0 / EO	0.05	<	5.05
	b_0 / EO	0.37	<	5.05
	b_1 / EO	0.00	<	5.05
	c_0 / EO	0.63	<	5.05
	CP / OP	0.86	<	9.28
4 Stations	a_0 / EO	0.17	<	5.05
	b_0 / EO	0.32	<	5.05
	b_1 / EO	0.21	<	5.05
	c_0 / EO	0.77	<	5.05
	CP / OP	0.75	<	9.28
3 Stations	a_0 / EO	0.06	<	5.05
	b_0 / EO	0.00	<	5.05
	b_1 / EO	1.63	<	5.05
	c_0 / EO	0.47	<	5.05
	CP / OP	0.19	<	9.28
2 Stations	a_0 / EO	0.14	<	5.05
	b_0 / EO	0.11	<	5.05
	b_1 / EO	0.15	<	5.05
	c_0 / EO	0.15	<	5.05
	CP / OP	0.11	<	9.28

For all cases, the null hypothesis are accepted which mean no significant difference between both datum constraints. Furthermore, Figure 17 until Figure 21 have visualised the similarity of the results (e.g. parameters correlation) obtained from both datum constraints for the case of minimum number of scan station (e.g. two scan stations). Additionally, the trend of the plotted graphs are quiet similar to the full network configurations.

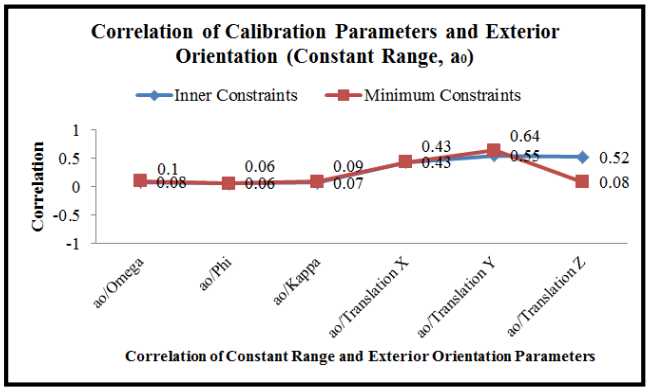

Figure 17 Parameter correlations of constant range and exterior orientation parameters (minimum stations configuration)

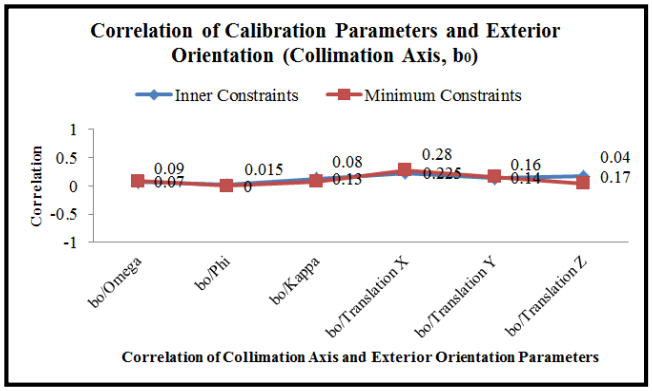

Figure 18 Parameter correlations of collimation axis and exterior orientation parameters (minimum stations configuration)

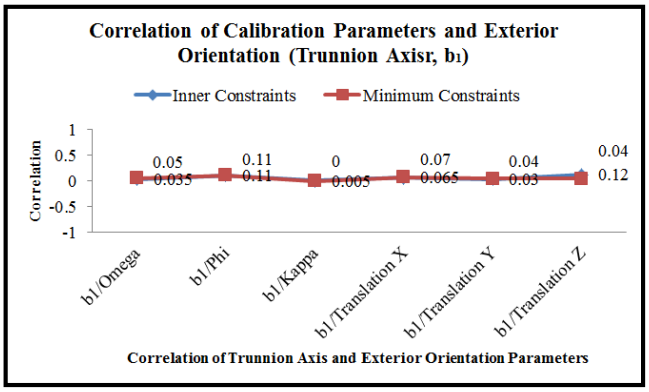

Figure 19 Parameter correlations of trunnion axis and exterior orientation parameters (minimum stations configuration)

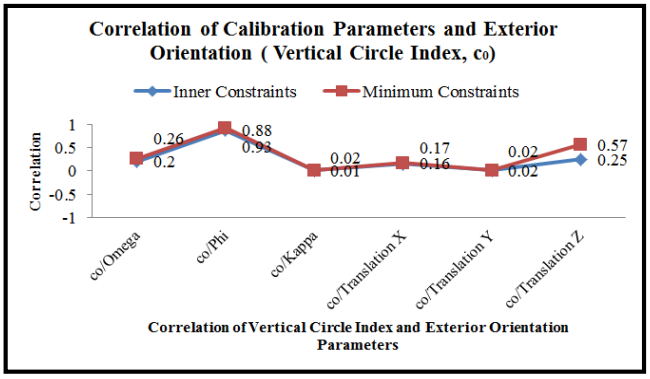

Figure 20 Parameter correlations of vertical circle index and exterior orientation parameters (minimum stations configuration)

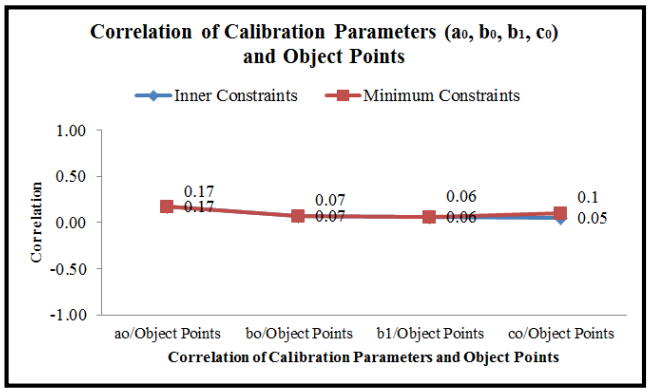

Figure 21 Parameter correlations of calibration parameters and object points (minimum stations configuration)

Through different surfaces configurations experiment, the datum constraints analysis was again performed. Outcomes of F-variance ratio test were organised in the Table VI for four different types of surfaces configurations. Values of calculated F for all circumstances have indicated the acceptance of null hypothesis, which also has increase the certainty of previous conclusion, there is no significant effect in datum constraints selection. Moreover, the minimum configuration for surfaces using two walls as illustrated in Figure 22 to Figure 26 does not indicated any obvious different between inner and minimum constraints, the graphs as well have similar trends as full network configuration.

Table VI F-variance ratio test for different surfaces configurations

Configuration	Parameter Correlations	Calculated F	>/<	Critical F
4 Walls	a_0 / EO	0.01	<	5.05
	b_0 / EO	0.25	<	5.05
	b_1 / EO	3.18	<	5.05
	c_0 / EO	0.61	<	5.05
	CP / OP	0.69	<	9.28
2 Walls and a Ceiling	a_0 / EO	0.01	<	5.05
	b_0 / EO	0.26	<	5.05
	b_1 / EO	1.60	<	5.05
	c_0 / EO	0.56	<	5.05
	CP / OP	0.31	<	9.28
3 Walls	a_0 / EO	0.00	<	5.05
	b_0 / EO	0.50	<	5.05
	b_1 / EO	0.81	<	5.05
	c_0 / EO	0.63	<	5.05
	CP / OP	0.40	<	9.28
2 Walls	a_0 / EO	0.00	<	5.05
	b_0 / EO	0.07	<	5.05
	b_1 / EO	0.40	<	5.05
	c_0 / EO	0.40	<	5.05
	CP / OP	0.02	<	9.28

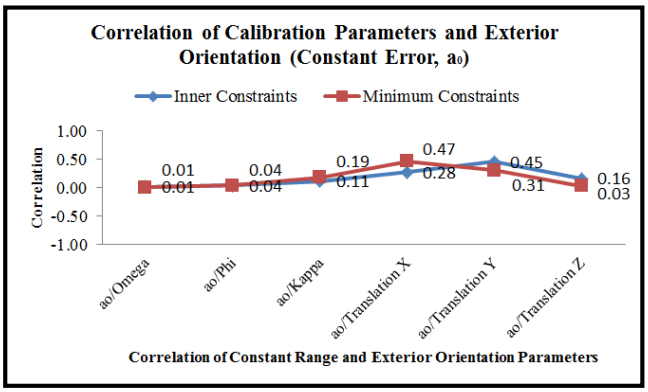

Figure 22 Parameter correlations of constant range and exterior orientation parameters (minimum surfaces configuration)

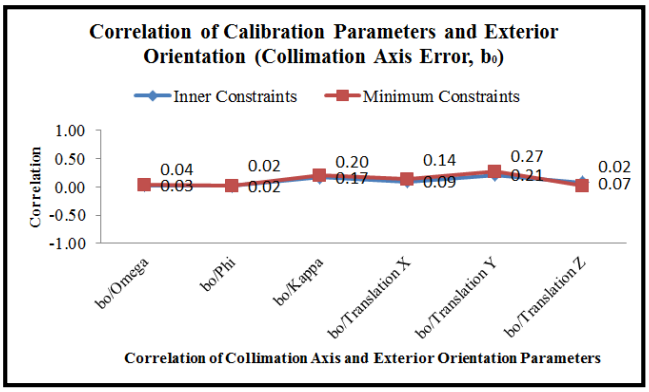

Figure 23 Parameter correlations of collimation axis and exterior orientation parameters (minimum surfaces configuration)

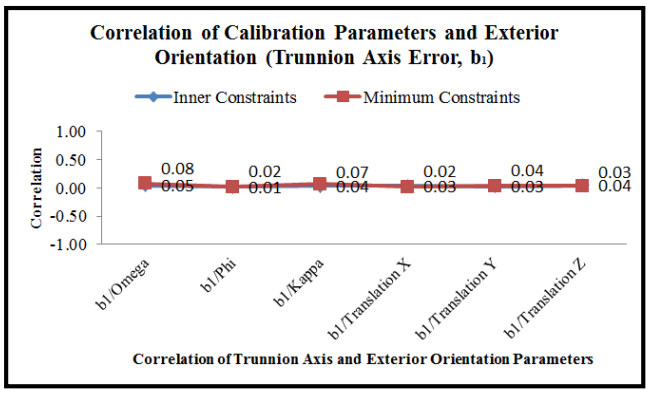

Figure 24 Parameter correlations of trunnion axis and exterior orientation parameters (minimum surfaces configuration)

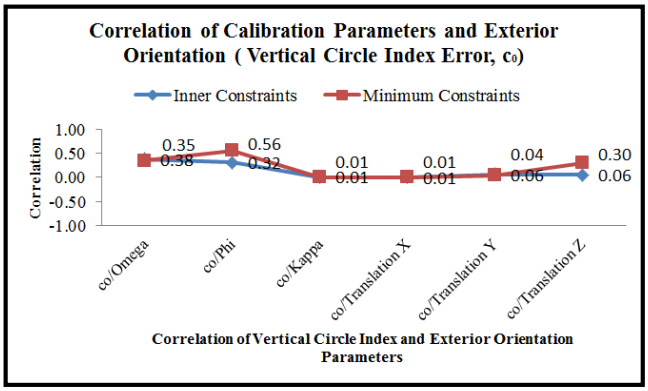

Figure 25 Parameter correlations of vertical circle index and exterior orientation parameters (minimum surfaces configuration)

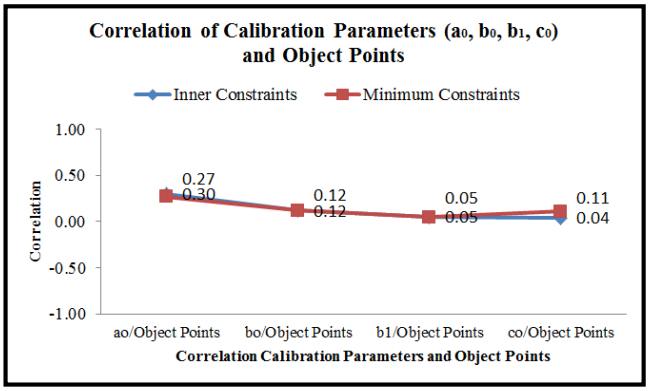

Figure 26 Parameter correlations of calibration parameters and object points (minimum surfaces configuration)

For the final configuration, different number of targets distribution, F-variance ratio test has concretely proved that there is no significant effect in parameter correlations from the datum constraints selection. As shown in Table VII, the null hypotheses have again statistically verified the significant similarity of both datum constraints. In addition, the trend depicted in Figure 27 to Figure 31 for minimum number of targets (e.g. 70% reduction or equivalent to 41 targets) have a similar shape as full network configuration.

Table VII F-variance ratio test for different targets configurations

Configuration	Parameter Correlations	Calculated F	>/<	Critical F
10% Targets Reduction	a_0 / EO	0.07	<	5.05
	b_0 / EO	0.20	<	5.05
	b_1 / EO	0.53	<	5.05
	c_0 / EO	0.61	<	5.05
	CP / OP	0.52	<	9.28
20% Targets Reduction	a_0 / EO	0.08	<	5.05
	b_0 / EO	0.27	<	5.05
	b_1 / EO	0.27	<	5.05
	c_0 / EO	0.61	<	5.05
	CP / OP	0.45	<	9.28
30% Targets Reduction	a_0 / EO	0.10	<	5.05
	b_0 / EO	0.39	<	5.05
	b_1 / EO	0.29	<	5.05
	c_0 / EO	0.62	<	5.05
	CP / OP	0.61	<	9.28
40% Targets Reduction	a_0 / EO	0.09	<	5.05
	b_0 / EO	0.28	<	5.05
	b_1 / EO	0.52	<	5.05
	c_0 / EO	0.56	<	5.05
	CP / OP	0.58	<	9.28
50% Targets Reduction	a_0 / EO	0.09	<	5.05
	b_0 / EO	0.27	<	5.05
	b_1 / EO	1.22	<	5.05
	c_0 / EO	0.55	<	5.05
	CP / OP	0.30	<	9.28
60% Targets Reduction	a_0 / EO	0.08	<	5.05
	b_0 / EO	0.18	<	5.05
	b_1 / EO	0.61	<	5.05
	c_0 / EO	0.56	<	5.05
	CP / OP	0.27	<	9.28
70% Targets Reduction	a_0 / EO	0.10	<	5.05
	b_0 / EO	0.14	<	5.05
	b_1 / EO	0.01	<	5.05
	c_0 / EO	0.71	<	5.05
	CP / OP	0.30	<	9.28

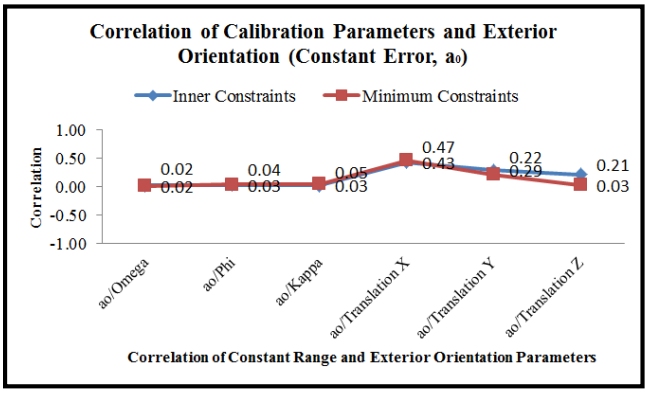

Figure 27 Parameter correlations of constant range and exterior orientation parameters (minimum targets configuration)

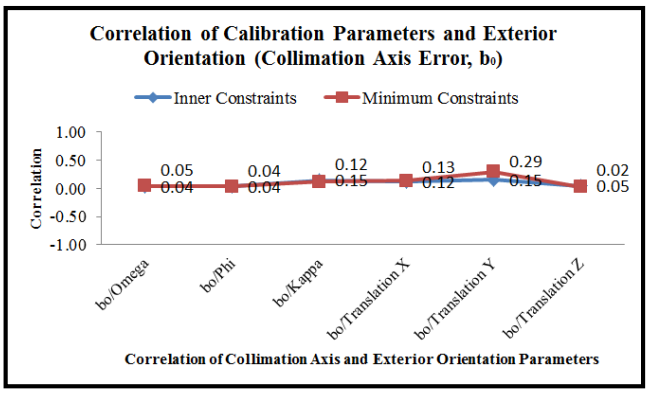

Figure 28 Parameter correlations of collimation axis and exterior orientation parameters (minimum targets configuration)

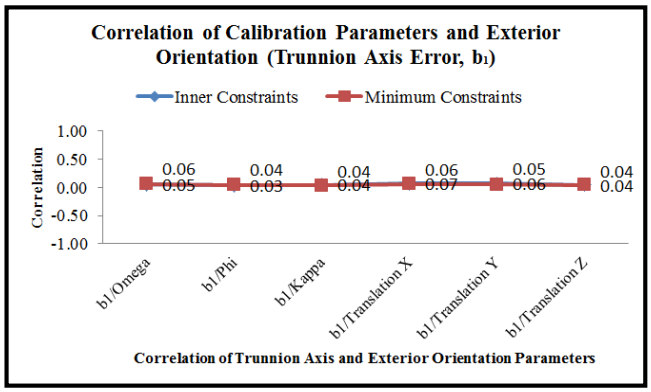

Figure 29 Parameter correlations of trunnion axis and exterior orientation parameters (minimum targets configuration)

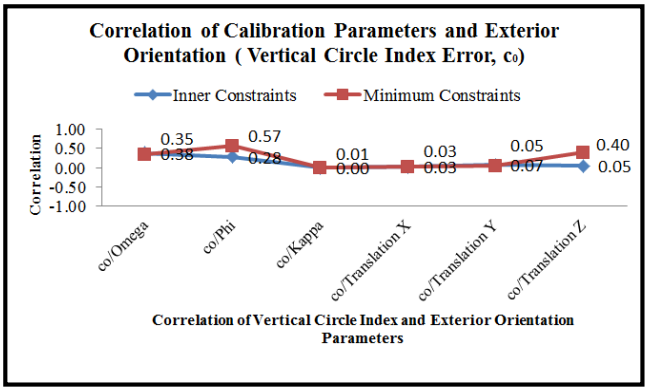

Figure 30 Parameter correlations of vertical circle index and exterior orientation parameters (minimum targets configuration)

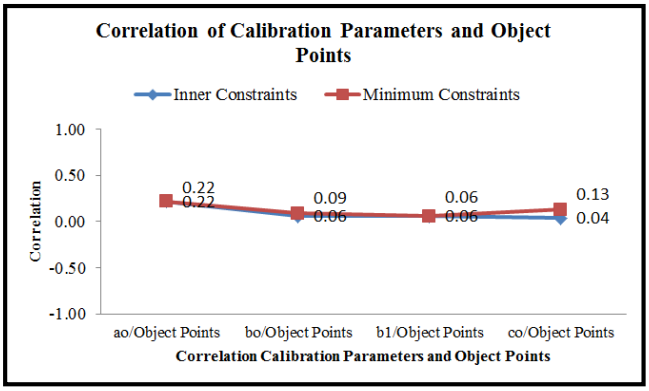

Figure 31 Parameter correlations of calibration parameters and object points (minimum targets configuration)

As discussed in Section 1, according to photogrammetry self-calibration, the used of inner constraints can increase the correlations between the calibration parameters and exterior orientations. Otherwise, employing minimum constraints tends to cause large correlations between object points and calibration parameters. However, trend in the graphs plotted (e.g. for full network, minimum stations, minimum surfaces and minimum targets configurations) indicates different assumption. Surprisingly, for all plotted graphs, the comparisons between the parameter correlations obtained from using both datum constraints are quite similar. Since the only causes for parameter correlation are network geometry and selection of datum constraints, thus, the outcomes of this study has graphically and statistically proved that the later cause is not relevant for TLS self-calibration. However, the network geometry should be made carefully, this is very crucial to ensure the quality of the results obtained (e.g. calibration parameters as well as to de-correlate the parameters).

6.0 CONCLUSION

A self-calibration procedure used for TLS calibration was originally adapted from photogrammetry technique, however the photogrammetry network configuration is not suitable for TLS application. This is due to the observables and measurement technique implemented by both photogrammetry and TLS are different. Therefore, further investigation was carried out to evaluate whether similar effect in datum constraints selection for photogrammetry is relevant for TLS. Graphical and statistical analyses were employed to examine any significant differences in the parameter correlations obtained from inner or minimum constraints. To ensure that the investigation is thoroughly executed, the datum constraints analyses were carried out using three variant network configurations: 1) minimum number of scan stations, 2) minimum number of surfaces for targets distribution, and 3) minimum number of point targets. The datum constraints analyses for all network configurations have indicated that the selection of datum constraints does not affect the values of parameter correlations. Both inner and minimum constraints can provide significantly similar parameter correlations. Nevertheless, the network configuration is a very crucial procedure to ensure that the correlation between the calculated parameters can be reduced.

Acknowledgement

The present research was made possible through a Vote 00G23 under UTM research grant GUP Flagship by Universiti Teknologi Malaysia (UTM). Special thanks goes to Ministry of Higher Education (MoHE) and Photogrammetry & Laser Scanning Research Group, INFOCOMM Research Alliance, UTM for the facility and technical support in this project.

References

[1] Syahmi, M. Z., Wan Aziz, W. A., Zulkarnaini, M. A., Anuar, A. and Othman, Z. 2011. The Movement Detection on the Landslide Surface by Using Terrestrial Laser Scanning. *Control and System Graduate Research Colloquium (ICSGRC)*, 2011 IEEE, Shah Alam, Selangor.

[2] Wan Aziz, W. A., Khairul, N. T. and Anuar. 2012. A. Slope Gradient Analysis at Different Resolution Using Terrestrial Laser Scanner. *Signal Processing and its Applications (CSPA)*, 2012 IEEE 8th International Colloquium, Melaka.

[3] Gordon, S. J. and Lichti, D. D. 2007. Modeling Terrestrial Laser Scanner Data for Precise Structural Deformation Measurement. *ASCE Journal of Surveying Engineering*. 133 (2): 72-80.

[4] Rönnholm, P., Nuikka, M., Suominen, A., Salo, P., Hyyppä, H., Pöntinen, P., Haggrén, H., Vermeer, M., Puttonen, J., Hirsi, H., Kukko, A., Kaartinen, H., Hyyppä, J. and Jaakkola. 2009. A. Comparison of Measurement Techniques and Static Theory Applied to Concrete Beam Deformation. *The Photogrammetric Record*. 24(128): 351-371.

[5] González-Aguilera, D. Gómez-Lahoz, J., Sánchez, J. 2008. A New Approach for Structural Monitoring of Large Dams With a Three-dimensional Laser Scanner. *Sensors*. 8(9): 5866-5883.

[6] González-Jorge, H., Riveiro, B., Arias, P., and Armesto, J. 2012. Photogrammetry and Laser Scanner Technology Applied to Length Measurements in Car Testing Laboratories. *Measurement*. 45: 354-363.

[7] Riveiro, B., González-Jorge H., Varela, M., and Jauregui, D. V., 2013. Validation of Terrestrial Laser Scanning and Photogrammetry Techniques For The Measurement Of Vertical Underclearance And Beam Geometry In Structural Inspection Of Bridges. *Measurement*. (46): 184-794.

[8] Lichti, D. D. 2007. Error Modelling, Calibration and Analysis of an AM-CW Terrestrial Laser Scanner System. *ISPRS Journal of Photogrammetry & Remote Sensing*. 61: 307-324.

[9] Brian, F., Catherine, L. C. and Robert, R. 2004. Investigation on Laser Scanners. *IWAA2004*, 2004 CERN, Geneva.

[10] Mohd Azwan, A., Halim, S., Zulkepli, M., Albert K. C., Khairulnizam, M. I. and Anuar, A. 2013. Calibration and Accuracy Assessment of Leica ScanStation C10 Terrestrial Laser Scanner. Development in Multidimensional Spatial Data Models, *Springer Lecture Notes in Geoinformation and Cartography (LNG&C)*, March 2013. 33-47.

[11] Reshetyuk, Y. 2009. Self-Calibration and Direct Georeferencing in Terrestrial Laser Scanning. *Doctoral*

Thesis in Infrastructure, Royal Institute of Technology (KTH), Stockholm, Sweden, 2009.
[12] Fraser, C. S. 1996. *Network Design. In Close Photogrammetry and Machine Vision*. Edited by K. B. Atkinson. Whittles Publishing, Roseleigh House, Latheronwheel, Scotland, UK. 256-279.
[13] Lichti, D. D. 2010. A Review of Geometric Models and Self-Calibration Methods for Terrestrial Laser Scanner. *Bol. Ciênc. Geod., sec. Artigos*, Curitiba. 3-19.
[14] Lichti, D. D., Chow, J. and Lahamy, H. 2011. Parameter De-Correlation and Model-Identification in Hybrid-Style Terrestrial Laser Scanner Self-Calibration. *ISPRS Journal of Photogrammetry and Remote Sensing.* 66: 317-326.
[15] Schneider, D. 2009. Calibration of Riegl LMS-Z420i based on a Multi-Station Adjustment and a Geometric Model with Additional Parameters. *The International Archives of the Photogrammetry, Remote Sensing and Spatial Information Sciences*. 38 (Part 3/W8): 177-182.
[16] Gielsdorf, F., Rietdorf, A. and Gruendig, L. 2004. A Concept for the Calibration of Terrestrial Laser Scanners. *TS26 Positioning and Measurement Technologies and Practices II-Laser Scanning and Photogrammetry*. FIG Working Week 2004, Athens, Greece. 1-10.
[17] Abdul, W. I. and Halim, S. 2001. *Pelarasan Ukur*. Kuala Lumpur: Dewan Bahasa dan Pustaka. 5-9.
[18] Gopal, K. K. 1999. *100 Statistical Test. Thousand Oaks*, California: SAGE Publications Ltd. 37-38.